Proceedings of the 28th IEEE
EMBS Annual International Conference
New York City, USA, Aug 30-Sept 3, 2006

Textural Assessment in Digital Mammograms

F.E. Trujillo-Zamudio, J. Márquez, Y. Villaseñor and M.E. Brandan

***Abstract*—This work focuses on testing textural and morphological parameters to assess characteristic features of digital mammograms. The selected images were radiological studies from the Instituto Nacional de Cancerología in Mexico City, evaluated as BI-RADS 4 or 5, meaning "probably malign" or "malign" findings, respectively. All patients were subjected to a biopsy procedure after the image was taken. The study group consisted of patients diagnosed with cancer, while the control group included those without cancer. We propose to analyze textural roughness by the mean height-width ratio of extrema (MHWRE) and morphological features by circularity. Results shows good differentiation (correct diagnosis) for 46% of the images, bad differentiation (wrong diagnosis) for 25%, and undetermined diagnosis for 29% of the cases.**

I. Introduction

IN the United States, each year, an average of 43000 women will present breast cancer [1]. In Mexico, breast cancer is the second cause of women's death by cancer [1]. Mammographic images are 2D projections whose gray levels represent the attenuation and scatter suffered by the X rays when traversing the breast. The term radiographic density refers to the radio- opaqueness of a tissue, a large density corresponding to a white radiographic image. A first approach to qualify mammograms according to the radiographic density was the Wolf scheme [2]-[3], aimed at finding a correlation between density and cancer risk, but the technique lacked objectivity due to intra- and inter-observer variations. Recently, researchers have studied intensity-histogram features and applied threshold techniques and fractal characteristics to analyze radiographic density in digital images [4]-[8]. An alternative approach would be to analyze morphology and texture features of mammograms, but to our knowledge, no satisfactory results have been reported to date.

Our objective is to assess characteristic texture and morphological features related to breast cancer in digital mammographic images by means of a global analysis. These features might help to detect breast cancer disease and reduce unnecessary biopsy procedures. In this work we report our current experiences with texture roughness and morphological measurements, which are related to anatomical features of normal and pathological tissue in radiological projections of the breast.

Manuscript received April 24, 2006.

F.E. Trujillo-Zamudio was with the Instituto de Física, UNAM, México. A.P. 20-364, 01000. He is now with the Instituto Nacional de Cancerología A.P. 14080 D.F., Mexico (e-mail: flaviotrujillo@gmail).

J. Márquez is with CCADET, UNAM, A.P 70-186, 04510 D.F., Mexico (e-mail: marquez@aleph.cinstrum.unam.mx).

Y. Villaseñor is with the Instituto Nacional de Cancerología A.P. 14080 D.F., Mexico.

M.E. Brandan is with the Instituto de Física, UNAM, México. A.P. 20-364, 01000. (e-mail: brandan@fisica.unam.mx).

II. Methodology

Our research focused on digital mammographic craneo-caudal images of patients from the *Instituto Nacional de Cancerología,* in Mexico City. The selected studies had been evaluated as BI-RADS 4 or 5, meaning "probably malign" or "malign" findings, respectively; all the patients were subjected to a biopsy procedure after the image was obtained. The study group comprised 24 patients diagnosed with cancer, while the control group consisted of 78 patients without cancer. First, we defined a training phase to analyze texture (*mean height/width ratio of extrema*) and morphology (*contour circularity*) in 18 images from the study group and 18 images from the control group. With these results we fed a program to obtain parameter values suggesting malignancy or benign disease. Next, in a validation phase, we used the program to analyze all images to evaluate the method performance in assigning a correct diagnosis, either of breast cancer or benign disease.

A. Texture feature: Mean height/width ratio of extrema (ρ)

To quantify breast texture in mammograms, we propose, as a textural roughness measurement, the mean height/width ratio of extrema (ρ), which has been tested to characterize textures arising from partially-organized structures in cell-proliferation studies [8]. Similarities in texture appearance have prompted us to test this feature on digital mammographies, by considering one-dimensional scans (signal profile samples) from an image. A "texture signature" is obtained from the height-to-width ratios of all intensity peaks in sample profiles from the image. A single peak on a profile can be characterised by depth or height (grey-level intensity) and width (separation between extrema). We have measured horizontal (width) and vertical (height) projections of vectors ξ y ζ at each peak of the profile (Fig. 1). For a peak (or valley), its height is $(\xi^{\perp} + \zeta^{\perp})/2$ and width is $(\xi^{\parallel} + \zeta^{\parallel})$; and there are N one-dimensional extrema ("roughs") of the texture (either valleys or peaks). The mean of the N height/width ratios in a single profile is called MHWRE. If NM is the number of profiles in an image, the mean of the NM MHWRE is called the mean height/width ratio of extrema of image, and referred here as ρ.

Calculations are performed only if the following conditions are met: a) the ratio minimum/maximum vertical

peak projections is greater than 0.6 (approximate value where the human eye distinguishes a roughness feature in textural images) and, b) the peak height (the average of the two vertical projections) is greater than a pre-established threshold of noise, η. The parameter ρ is defined in equations (1-3)

$$\rho = \frac{1}{\mathrm{NM}} \sum_{i=1}^{\mathrm{NM}} \mathrm{MHWRE}_i \tag{1}$$

$$MHWRE = \frac{1}{N} \sum_{i=1}^{N} w_i R_i \tag{2}$$

where $$R_i = \frac{\left(\xi_i^{\perp} + \zeta_i^{\perp}\right)/2}{\xi_i^{\parallel} + \zeta_i^{\parallel}}$$

and (3)

$$w_i = \begin{cases} 1 & \text{if } \dfrac{\min(\xi_i^{\perp}, \zeta_i^{\perp})}{\max(\xi_i^{\perp}, \zeta_i^{\perp})} > 0.6 \quad \& \quad (\xi_i^{\perp} + \zeta_i^{\perp})/2 > \eta \\ 0 & \text{otherwise} \end{cases}$$

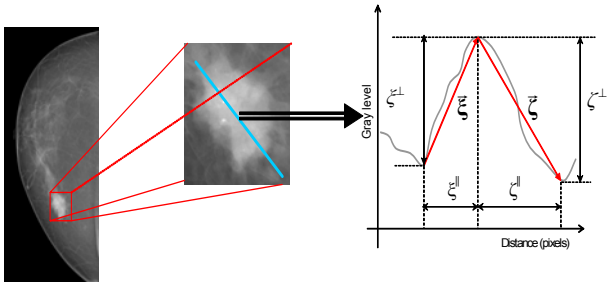

Fig. 1. Left: A mammogram. Center: Example of a mammogram region. Right: Parameters used to define the peak height/width ratio of extrema.

B. *Morphological feature: Circularity (k)*

We propose to analyze morphological features with circularity measurements. Some authors [9] have defined a normalized measure of circularity of a region as the (Perimeter)^2/Surface ratio, measured in pixels. We have used a measure κ of circularity defined as:

$$\kappa = \frac{4\pi A}{P^2}, \tag{4}$$

where P is the perimeter of a region and A, its surface (all in pixels). With κ defined in this way the iso-density structures with irregular borders present on malignant breast tissue will have a small κ compared with normal tissue. An example of the use of this parameter is show in figure 2.

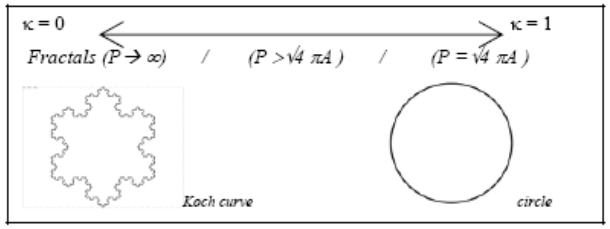

Fig. 2. Scale of κ value for two kinds of morphological shapes

III. Training Phase Results

A. *Mean height/width ratio of extrema (ρ)*

Results for ρ in cancer images are for η=10 (ρ_{10}) and η=100 (ρ_{100}) (in pixel intensity). We have chosen a small (10) and a large (100) gray level threshold for η, to analyze "soft texture" and "rough texture", respectively. There is no significant difference of mean value and standard deviation for ρ_{10} and ρ_{100} in cancer images, where $\langle\rho_{10}\rangle$=10.96±.2.75, $\langle\rho_{100}\rangle$ = 17.30±.7.87, $\langle\sigma_{\rho 10}\rangle$ = 3.03±2.60, and $\langle\sigma_{\rho 100}\rangle$ = 9.56±4.31. Whenever ρ is larger, the appearance is of greater roughness. Mean standard deviation of ρ, that is $\langle\sigma_{\rho}\rangle$, shows the variance in texture. Results for benign images show a similar behavior.

In Figs. 3 and 4 we show the variation of the textures ρ_{10} and ρ_{100} in each image, respectively.

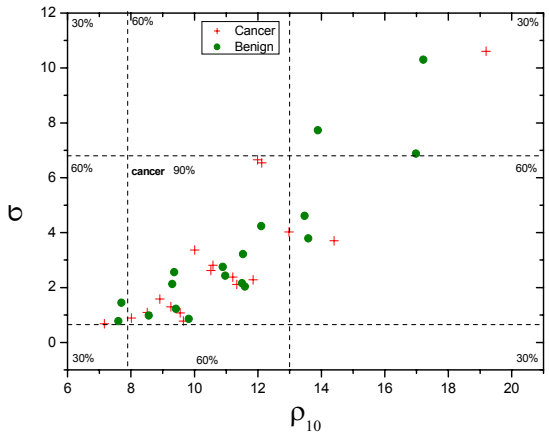

Fig. 3. Training phase images: $\sigma_{\rho 10}$ vs. ρ_{10}

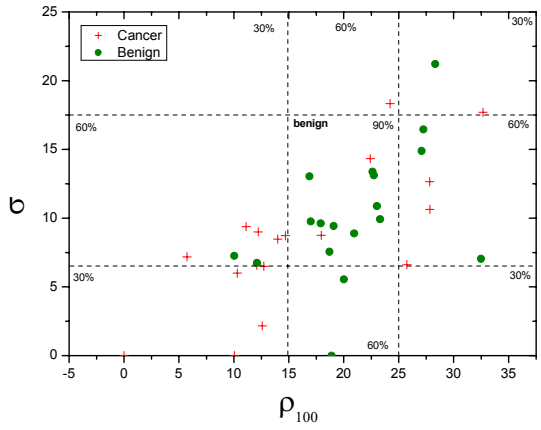

Fig. 4. Training phase images: $\sigma_{\rho 100}$ vs. ρ_{100}.

In Fig. 3 in order to differentiate between cancer and benign images, a simple, linear classification criterion was used. To this end, the scatter plot is divided in 9 regions, assigning to each one an intuitive percentage of malignancy, since the central section contains mainly cancer images. Cancer and benign regions turned out to be complex shaped, thus, a linear separation is not enough.

In Fig. 4, we have also tried a linear separation, resulting

in a central section mainly with benign images. This time, the linear-separation criterion offers a better classification of both groups of images.

B. *Circularity (k)*

There is no significant difference in $<\kappa>$: $<\kappa>_{cancerr}=0.046\pm0.015$ versus. $<\kappa>_{benign}= 0.044\pm0.030$. However, the mean standard deviation of κ for images with cancer is approximately twice the one from images with benign lesions: $<\sigma_\kappa>_{cancer}=0.020\pm0.014$ vs. $<\sigma_\kappa>_{benign}=0.013\pm0.013$.

Figure 5 shows the variation of parameter κ in each image for the training group. When trying again a linear classification, we find mainly cancer images in the central section.

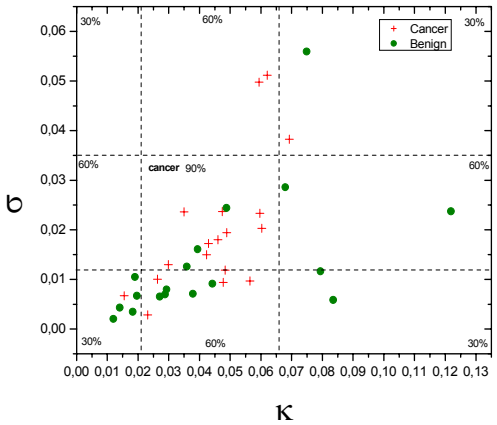

Fig. 5. Training phase images: σ_κ vs. κ

IV. Discussion

A. *Discussion of the Training phase*

To obtain correlated information from the three plots (Figs. 3-5), we have plotted the data in a 3D-feature space.

Fig. 6 shows that a linear classification criterion performs better, in both groups, with the ρ_{100} and κ features. In this way, we have divided the space of Fig. 6 in nine blocks, each one with an intuitive possibility of containing cancer images. Intervals are defined as:

$\kappa = [0.02;0.8]$ & $\rho_{10} = [0;15]$	90%
$\kappa = [0.02;0.8]$ & $\rho_{100} = (15;25]$	30%
$\kappa = [0;0.02)U(0.08;1]$ & $\rho_{100} = [0;25)$	30%
$\rho_{100} = (25;50]$	60%

Considering the results presented in Figs. 4-6, we propose an image classification by means of a scoring system. That is, each image will be analyzed and assigned a classifying score equal to the sum of percentages from Figs. 2-4 (double weight to Figs. 3 and 4). Each class represents a possibility (in percent) of malignancy. With this scoring system, the lowest classification is 1.5, representing 30% of malignancy, and the highest is 4.5, representing 90% of malignancy.

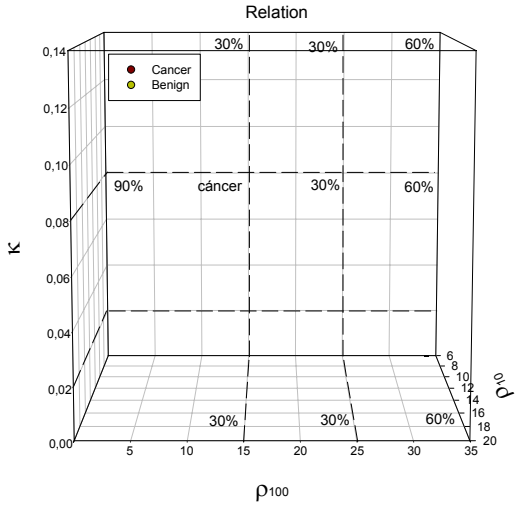

Fig. 6. Relation among ρ_{10}, ρ_{100} and κ features

B. *Validation phase*

In Fig. 7 we present results for 102 images (24 cancer and 78 benign lesions) in a 3D-feature space, similar to Fig. 6. The results of the scoring analysis are presented in Table 1. The training group comprised 18 cancer and 18 benign images. The validation group comprised 6 cancer and 60 benign images.

TABLE I
TRAINING AND VALIDATION PHASES: PERCENTAGE OF GOOD, BAD AND UNDETERMINED CLASSIFICATION OF MAMMOGRAPHIC IMAGES

Classification	Training		Validation	
	Cancer	Benign	Cancer	Benign
Good	61	39	50	42
Bad	11	17	17	32
Undetermined	28	44	33	25

Results are in percentage.

Results in Table I show that the training phase has reached 61% of good classifications of cancer images, and 39% of good classifications for benign images. A possible explanation for the poorer performance with benign images is that the scoring system was defined to accurately evaluate the cancer images. In this case, an important percentage of benign images have been undetermined.

Results for the validation group in Table 1 show a lower percentage of good classification. This result is not significant because of the relatively small number of available images for this (preliminary) study. Considering the benign images, their percentage of good classification is higher than in the training phase, and this is a more significant result since this validation group had three times more images than the training group.

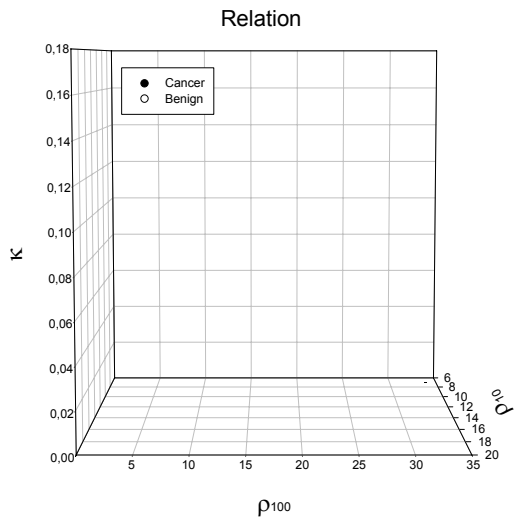

Fig. 7. Relation among ρ_{10}, ρ_{100} and κ for the 102 images (24 cancer and 78 benign images).

Table II presents final results, considering the scoring system for classification of all analyzed mammograms: 24 cancers and 78 benign lesions.

TABLE II
PERCENTAGE OF GOOD, BAD AND UNDETERMINED CLASSIFICATION

Global Results in percentage

Classification	Cancer	Benign
Good	58	42
Bad	13	28
Undetermined	29	29

Table II indicates a good classification of 58% of 24 cancer images, 13% wrong assessments and 29% of undetermined classification (same percentage for cancer and benign disease). For 78 benign images, 42% of adequate classification, 28% of wrong assessment and 29% of undetermined classification has been obtained.

Analyzing Table II and considering all 102 images (cancer and benign disease), 46% of good assessment, 25% of bad assessment and 29% of undetermined classification has been reached. This means that for each 10 images, this system will classify adequately 4 (or 5) images, inadequately 3 (or 2), and 3 images will remain undetermined.

V. CONCLUSIONS

We have analyzed 102 mammographic images of patients, 24 with cancer and 78 with benign breast disease. We have extracted the mean height/width ratio of extrema ρ as textural feature, and the circularity κ as characterization of morphology. The results show that for each 10 images, the proposed system will classify adequately 4 (or 5) images, inadequately 3 (or 2) images and 3 images will be undetermined.

Our objective was to assess characteristic texture and morphological features related to breast cancer in digital mammographic images, which might help to detect breast cancer disease and reduce unnecessary biopsy procedures. This goal has been partially achieved. The presented results are not yet satisfactory for clinical use, and other textural and morphological features from digital mammograms need to be assessed.

This study is a first step towards an automated classification system which might assist the quantitative clinical evaluation of digital mammograms.

REFERENCES

[1] *The World Health Organisation* (WHO) databank. http://www-depdb.iarc.fr/who/menu.htm.

[2] J.N. Wolfe, "Breast patterns as an index of risk of developing breast cancer". *Am. J. Roentgenol*, 126, pp. 1130-1139, 1976.

[3] J.N. Wolfe, "Risk for Breast Cancer Development determined by mammographic parenchymal pattern". *Cancer*, 37, pp. 2486-2492, 1976.

[4] J.W. Byng, M.J. Yaffe, G.A. Lockwood, L.E. Little, D.L. Tritchler, N.F. Boyd, "Automated analysis of mammographic densities and breast carcinoma risk". *American Cancer Society*, 80(1), pp. 66-74, 1997

[5] J.W. Byng, M.J. Yaffe, R.A. Jong, R.S. Shumak, G.A. Lockwood, D.L. Tritchler, N.F. Boyd, "Analysis of mammographic density and breast cancer risk from digitized mammograms". *InfoRad,*, 18(6), pp. 1587-1598, 1998.

[6] M.J. Yaffe, N.F. Boyd, J.W. Byng, R.A. Jong, E. Fishell, G.A. Lockwood, L.E. Little, D.L. Tritchler, "Breast cancer risk and measured mammographic density". *Eur. J. Cancer Prev.*, Suppl 1, pp. 47-55, 1998.

[7] N.F. Boyd, G.A. Lockwood, L.J. Martin, J.W. Byng, M.J. Yaffe, D.L. Tritchler, "Mammographic density as a marker of susceptibility to breast cancer: a hypothesis", *IARC Sci. Pub*., 154, pp. 163-169, 2001.

[8] G. Corkidi, L. Vega, J. Márquez, E. Rojas, P. Ostrovsky-Wegman 1998. "A Roughness Feature of Metaphase Chromosome Spreads and Nuclei for Automated Cell Proliferation Analysis". *Medical and Biological Engineering and Computing*, 36(6), pp. 679-685, 1998.

[9] W. Qian, L. Li, and L.P. Clarke, *Image feature extraction for mass detection in digital mammography: influence of wavelet analysis*, Med.Phys., 26(3):402-408, 1999.